JACS
JOURNAL OF THE AMERICAN CHEMICAL SOCIETY

Article

pubs.acs.org/JACS

Bottom-Up Construction of POM-Based Macrostructures: Coordination Assembled Paddle-Wheel Macroclusters and Their Vesicle-like Supramolecular Aggregation in Solution

Yi Zhu,[⊥,†,§] Panchao Yin,[⊥,‡,¶] Fengping Xiao,[§] Dong Li,[‡] Emily Bitterlich,[‡] Zicheng Xiao,[§,†] Jin Zhang,[§] Jian Hao,[§] Tianbo Liu,*[,‡,¶] Yuan Wang,*[,†] and Yongge Wei*[,§,†]

[†]State Key Laboratory for Structural Chemistry of Unstable and Stable Species, College of Chemistry and Molecular Engineering, Peking University, Beijing 100871, P. R. China

[‡]Department of Chemistry, Lehigh University, Bethlehem, Pennsylvania 18015, USA

[§]Department of Chemistry, Tsinghua University, Beijing 100084, P. R. China

[¶]Department of Polymer Science, The University of Akron, Akron, Ohio 44325-3909, USA

Supporting Information

ABSTRACT: A bottom-up approach to obtain nanoclusters and large, uniform vesicle-like structures containing organic functionalized hexamolybdates in solution state were developed. Hexamolybdate functionalized carboxylic acid coordinated with two copper ions to form paddle-wheel tetrapolyoxometalate clusters with the features of macro-ions, which can spontaneously assemble into large, stable blackberry-type structures in suitable solvents, completing a hierarchical organization from small POM molecules to nanoscale complexes and then to supramolecular structures.

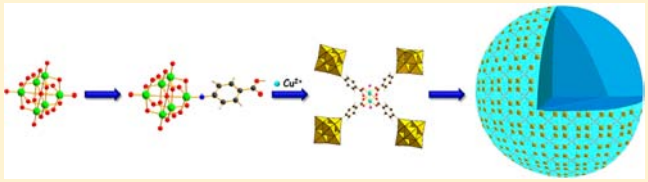

1. INTRODUCTION

The controllable and devisable organization from small molecules to macroscale aggregate structures, toward functional nanosystems and nanomachines with desired configurations and properties, defines one of the greatest challenges in contemporary chemistry.[1,2] With the so-called noncovalent synthetic strategy,[1g] the coordination-driven self-assembly has been proved to be a powerful and versatile paradigm to build up well-defined nanoscale arrangements with desirable shapes and controlled sizes in fewer synthetic steps, and fast and facile bench operation.[3,4] Among various molecular building blocks exploited in noncovalent synthesis, polyoxometalate-based (POM-based) subunits have gained increasing interest,[5−14] due to the diversity of structures and unique physical properties of POMs,[15,16] promising new approaches for the design and development of more functional macrostructures with potential application in catalysis, medicine, and photoelectronic materials. Furthermore, the noncovalent weak physical interactions are often responsible for the complicated supramolecular assemblies of polyelectrolytes, carbon nanotubes, macro-ions, and biomacromolecules.[17] Herein, we will report a unique hierarchical assembly strategy involving both coordination and noncovalent physical interactions successively, which results in the organization from small POM molecules to nanoscaled paddle-wheel complexes and then to blackberry-type assemblies.

To date, two coordination approaches have been developed for the assembly of POMs into macrostructures: (1) Transition metal-substituted POMs are chosen as subunits and organic ligands as intermolecular linkers through coordinating with transition metal ions.[9] However, as the transition metal-substituted POM subunits are generally formed under hydrothermal conditions, the structures of which are unpredictable, it is difficult to prepare the desired macrostructures from the starting materials in a predesigned manner. (2) Preformed organic derivatives of POMs, that is POM-functionalized organic ligands, are utilized as building blocks, and transition metal ions as linkers via a well-defined coordination mode.[10] Such a preparation process for macrostructures is more designable. Despite its high efficiency and importance, reports on such an approach are extremely rare, and only a few well-defined examples are obtained.[11−14] Thanks largely to the pioneering work of Hill,[11] several macrostructures based on hexavanadate organic derivatives (carboxyl-capped hexavanadate and bis(pyridyl)-capped hexavanadate) coordinating with transition metal ions have been successfully obtained via this approach. Cronin[12] and Hansenknopf[13] focused on the coordination chemistry of organic functionalized Anderson POMs, with which they had developed the cell-selective adhesion material and gels with birefringence properties. Moreover, Peng and coworkers[14] have used hexamolybdate derivatives bearing a terpyridine terminus to coordinate with a

Received: August 14, 2013
Published: October 10, 2013

   dx.doi.org/10.1021/ja408228b | J. Am. Chem. Soc. 2013, 135, 17155−17160

transition metal ion to create electric-active structures, the crystal structures of which are not obtained, unfortunately.

In this work, we chose organoimido-derivatized hexamolybdate containing a carboxyl terminus, $(Bu_4N)_2[O_{18}Mo_6{\equiv}NC_6H_4\text{-}4\text{-}COOH]$ (**1**),[18] as subunits and Cu^{2+} as the coordinating transition metal ion on basis of the following design considerations: (1) Carboxylate is an efficient ligand in chelating Cu^{2+}, and its coordination chemistry has been well developed. We especially know much about the equilibrium of the coordination reaction. Thus, we can control the assembly and disassembly of the macrostructure through adapting the environment of its solution, and finally the size and charge of the anions in the solution are adaptable in that way. Since Liu mentioned in his work that size and charge of POMs are important factors in forming blackberry-like structures,[7] our research might be a good candidate for systemically studying such effects. (2) Cu^{2+}-carboxylate coordination mode usually adopts a discrete binuclear paddle-wheel motif,[19] which is a very useful building block to make self-assembled metal organic polyhedra.[3e,4c,d] It might provide us a way to obtain soluble assembly units. What is more important, the units can retain the structure in solution. Thus, it is predictable the macrostructure will form an interesting huge paddle-wheel tetrapolyoxometalate cluster with the binuclear copper unit as the center and hexamolybdates as blades. Such a giant macroion may exhibit some properties that the subunits do not possess.

2. EXPERIMETAL SECTION

Synthesis of Compound 1. A mixture of $(Bu_4N)_4[Mo_8O_{26}]$ (6.46 g, 3.0 mmol), DCC (1.36 g, 6.6 mmol) and *p*-aminobenzoic acid hydrochloride (0.696 g, 4.0 mmol) was refluxed in anhydrous acetonitrile (20 mL) at 110 °C for about 10 h. When the reaction mixture dissolved instantly in anhydrous acetonitrile at room temperature, the solution turned orange red. During the course of the reaction, its color changed to deep red, and some white precipitates (*N*,*N*-dicyclohexylurea) formed. When the resulting deep-red solution was cooled to room temperature, the white precipitates were removed by filtration. While the acetonitrile evaporated slowly in the open air, the product deposited as orange crystals (2.46 g, yield 42% based on Mo).

Synthesis of Compound 2. Compound **1** $(Bu_4N)_2[O_{18}Mo_6{\equiv}NC_6H_4\text{-}4\text{-}COOH]$ (0.0294 g, 0.02 mol) was dissolved in anhydrous acetonitrile (2 mL). $Cu(CH_3COO)_2{\cdot}5H_2O$ (0.02 g, 0.1 mmol) was dissolved in anhydrous acetonitrile (10 mL). One milliliter of solution was withdrawn and dropped into the compound **1** solution. The green block crystals (0.006 g, yield 20% based on compound **1**) were obtained by diffusion of Et_2O into the mixed solution.

Single-Crystal X-ray Diffraction. Single-crystal X-ray diffraction studies of compounds **1** and **2** were carried out using a Rigaku RAXIS-RAPID IP and a Rigaku CrystalClear CCD diffractometer, respectively. The data collection was performed at 293 and 81 K for compounds **1** and **2**, respectively, with Mo Kα radiation (λ = 0.71073 Å), operating respectively at 50 kV and 30 mA. Data reduction was performed by Rigaku RAPID AUTO ver 2.30 and CrystalClear for compounds **1** and **2**, respectively. The structures were both solved by direct methods and refined by the full-matrix least-squares method on F^2 with the SHELXTL software package of version 5.10.

Static Light Scattering. A commercial Brookhaven Instrument LLS spectrometer equipped with a solid-state laser operating at 532 nm was used for measurement of both SLS and DLS. SLS experiments were performed at scattering angles (θ) between 20 and 100°, at 2° intervals. However, due to the large fluctuations in scattered intensities at low scattering angles, we removed the data from 20 to 40° in the final analysis. Derived from the Rayleigh–Gans–Debye equation, a partial Zimm plot was used to analyze the SLS data to obtain the radius of gyration (R_g). The partial Zimm plot stems from the following approximate formula: $1/I = C(1 + R_g^2q^2/3)$. Here R_g is determined from the slope and the intercept of a plot of $1/I$ vs q^2.

Dynamic Light Scattering. DLS measures the intensity–intensity time correlation function by means of a BI-9000AT multichannel digital correlator. The field correlation function $|g^{(1)}(\tau)|$ was analyzed by the constrained regularized CONTIN method to yield information on the distribution of the characteristic line width Γ from $|g^{(1)}(\tau)| = \int G(\Gamma)\ e^{-\Gamma\tau}\ d(\Gamma)$.The normalized distribution function of the characteristic line width, $G(\Gamma)$, so obtained, can be used to determine an average apparent translational diffusion coefficient, $D_{app} = \Gamma/q^2$. The hydrodynamic radius R_h is related to D via the Stokes–Einstein equation: $R_h = kT/(6\pi\eta D)$ where k is the Boltzmann constant and η the viscosity of the solvent at temperature T. From DLS measurements, we can obtain the particle-size distribution in solution from a plot of $\Gamma G(\Gamma)$ vs R_h. The R_h of the particles is obtained by extrapolating $R_{h,app}$ to zero scattering angle.

Solution Preparation for Light-Scattering Studies. For a typical procedure, 2 mg of compound **2** crystalline sample was dissolved in 4 mL appropriate solvent (acetone/toluene mixed solvents). The obtained solutions were filtered with 200-nm pore size Millipore membrane filters and put into dust-free light-scattering sample vials.

Other Characterizations. UV–vis spectra were measured using a Lambda45 UV–vis spectrometer (Perkin-Elmer Intruments). Elemental analysis was performed on a Vario EL elemental analyzer. IR spectra were recorded with a Nicolet Magna-IR 750 spectrometer using KBr pellets. The ^{1}H NMR spectrum was taken on a Bruker ARX 400 NMR spectrometer at 298 K using DMSO-d_6 as solvent. The mass spectra were recorded using an ion trap mass spectrometer (Thermofisher LTQ). The TEM images were taken on a JEOL JEM-2000 electron microscope operated at 200 kV. Samples for the TEM analysis were prepared by dropping a small volume of the solution sample onto a holey carbon film on copper grid.

3. RESULTS AND DISCUSSION

The molecular structure of the carboxylic group functionalized organic POM cluster **1** is depicted in Figure 1. It was prepared

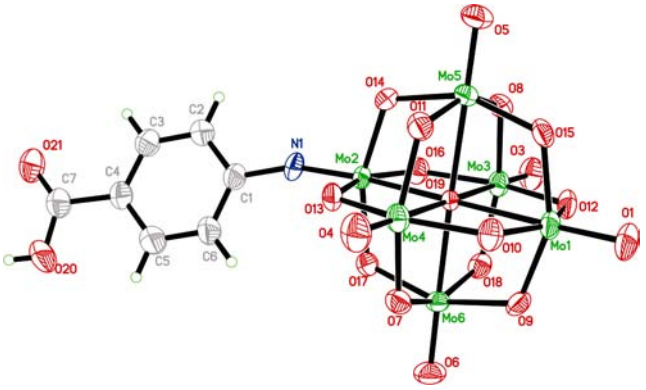

Figure 1. ORTEP viewing of the cluster anion of compound **1**. Non-hydrogen atoms were drawn at 50% thermal ellipsoid level.

by the well-developed imidoylization protocol:[20] a reaction of tetrabutylammonium α-octamolybdate and *para*-aminobenzoic acid hydrochloride in the presence of dicyclohexylcarbodiimide (DCC) in refluxed acetonitrile afforded compound **1** in ~40% yield. As shown in Scheme 1, the coordination self-assembly reaction of **1** with $Cu(CH_3COO)_2{\cdot}5H_2O$ produces the highly crystalline framework, $(Bu_4N)_{16}\{Cu_2(O_{18}Mo_6{\equiv}NC_6H_4\text{-}4\text{-}COO)_4{\cdot}(CH_3CN){\cdot}[(C_2H_5)_2O]\}$ (α) $\bullet\{Cu_2(O_{18}Mo_6{\equiv}NC_6H_4\text{-}4\text{-}COO)_4{\cdot}(CH_3CN)_2\}$ (β) (**2**), by diffusion of ethyl

dx.doi.org/10.1021/ja408228b | J. Am. Chem. Soc. 2013, 135, 17155–17160

Scheme 1. Coordination Assembly of POM-Functionalized Carboxylic Acid with Cu^{2+}

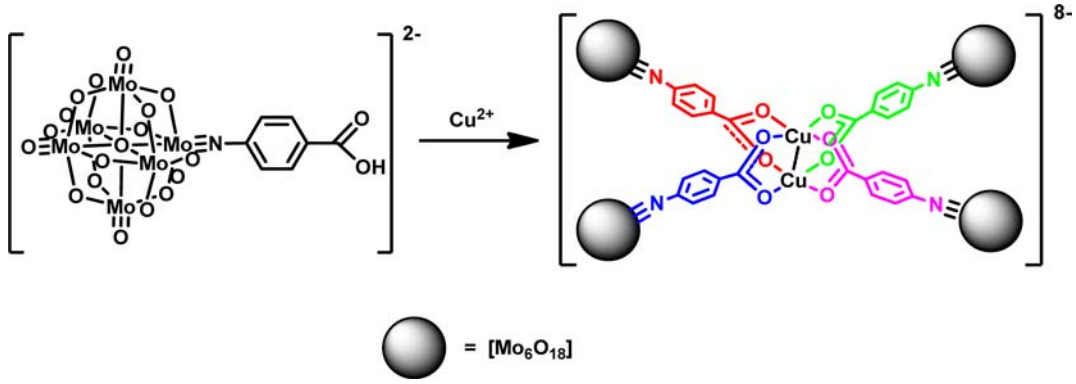

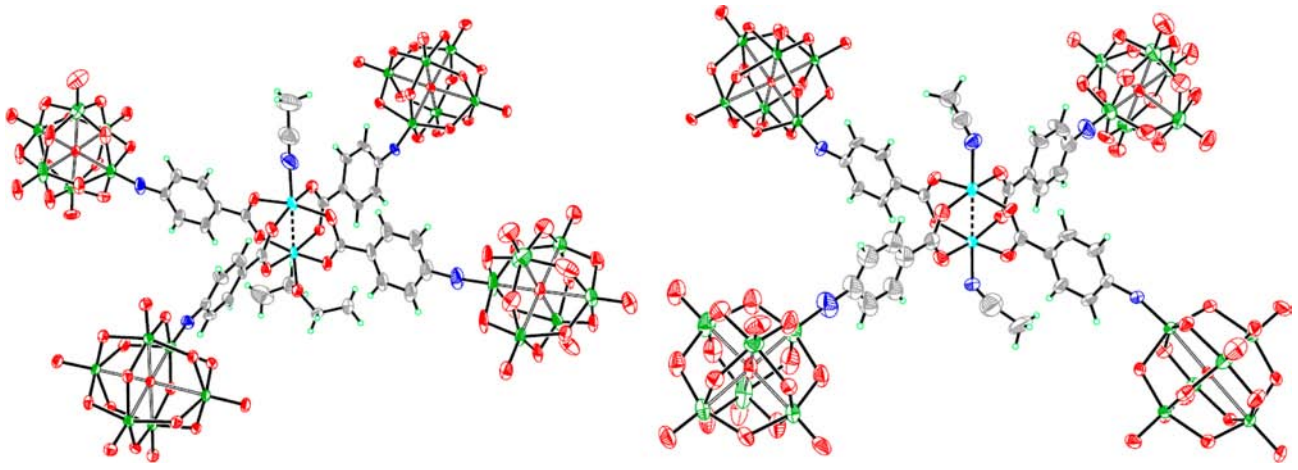

Figure 2. Molecular structure of **2*α*** (left) and **2*β*** (right). (Thermal ellipsoids were drawn at 30% probability level.) Atom coding: Cu (cyanine), Mo (green), N (blue), O (red), C (gray), H (greenish).

ether into a mixed solution of $(Bu_4N)_2[O_{18}Mo_6{\equiv}NC_6H_4$-4-COOH] and $Cu(CH_3COO)_2{\cdot}5H_2O$ (2:1) in acetonitrile.

Single-crystal X-ray diffraction investigation revealed that compound **2** crystallizes in triclinic space group $P\bar{1}$. Its molecular structure is presented in Figure 2. There are two very similar macro-anions in each asymmetric unit. As expected, both of the two anions present a paddle-wheel-like structure containing a dinuclear copper unit and four large hexamolybdate clusters with the length ranging from 13.277 to 13.537 Å. From bond valence sum (BVS) analysis,[21] the chemical valence of all the Cu ions is +2. Each Cu(II) ion is five-coordinated, with four carboxylate oxygens of the same carboxylate groups in equatorial positions with Cu···O distances in the range 1.939−1.968 Å, and two solvent molecules at the apex (for cluster α, the two solvent molecules are ethyl ether and acetonitrile; for the β cluster, both of the two solvent molecules are acetonitrile), completing the square pyramidal coordination geometry. The four POM functionalized carboxylates bridge both of the two copper ions to form a paddle-wheel-type supramolecule with the short Cu···Cu distance of 2.630(2) Å. The solvent−copper coordination distances are much longer than the Cu···O distances, which demonstrates that the coordination bond between solvent molecules and copper is weaker than the common coordination bond. The solvent molecules, thus, are easily replaced by other molecules, and that is the probable reason of the coexistence of α and β clusters.

Compound **2** exhibits characteristic bands of ν_{as}(COO) and ν_s(COO), appearing at 1620 cm^{-1} and 1466 cm^{-1} respectively. Compared with the ν_{as}(COO) band at 1715 cm^{-1} [ν(COOH) un-ionized] of compound **1**, the two bands indicate the loss of the −COOH proton. Since it is found that a $\Delta\nu_{COO}$ difference value of these two bands at approximately 150−170 cm^{-1} corresponds to the bridging bidentate mode of coordination of the carboxylic group,[22] the present Δ value of ∼154 cm^{-1} suggests the dicopper tetracarboxylates paddle-wheel structure, which is in accord with the result of X-ray structural analysis. Compound **2** also shows characteristic bands of monosubstituted organoimido hexamolybdates:[23,24] Mo−N bond-stretching vibration at 976 cm^{-1} as a shoulder peak; Mo−O_t stretching vibration at 953 cm^{-1}; Mo−O_b−Mo stretching vibrations at 796 cm^{-1}.

The UV−vis absorption spectra of compound **2** are characterized by two bands in Figure 3. The strong band at 351 nm (ε = 7.78 × 10^4 M^{-1} cm^{-1}), originating from the charge-transfer transition of the coordinated N atom to the molybdenum atom (LMCT),[25] which is the same as that of compound **1**, indicates that coordination of carboxyl with copper(II) has little influence on the charge-transfer transition. The weak and broad band at 690 nm (ε = 1.00 × 10^3 M^{-1} cm^{-1}), corresponding to a $d_{xz,yz} \rightarrow d_{x^2-y^2}$ transition, is characteristic for spectra of the pseudo-octahedral copper(II) compounds.[26] However, another characteristic band at ∼370 nm for bridged systems with antiferromagnetic interactions, deriving from the charge transfer transition $np\pi{\sim}\sigma_{x^2-y^2}$ between

dx.doi.org/10.1021/ja408228b | J. Am. Chem. Soc. 2013, 135, 17155−17160

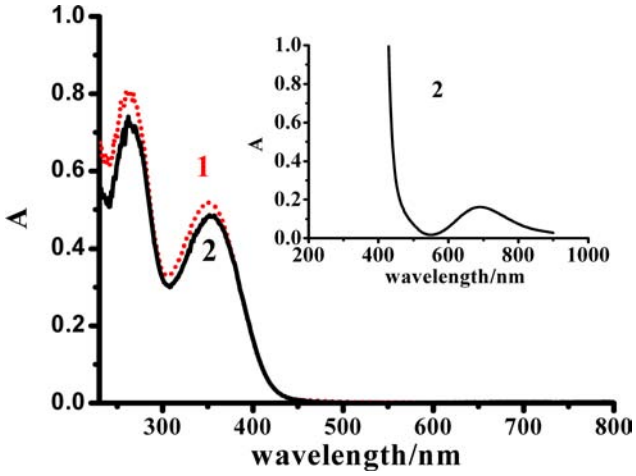

Figure 3. UV/vis absorption spectrum of compounds **1** and **2** in CH_3CN (6.42×10^{-6} M). (Inset) d–d transition for **2** in a more concentrated solution (1.75×10^{-3} M).

carboxylic oxygen atoms and the metal ion,[26] is not observed and may be overlapped by the strong band at 351 nm.

The electrospray mass spectrometry (ESI) shows two major isotopic clusters related to **2**, which strongly support our assumption that the macro-anions can exist in organic solvent. The signal at m/z 1272.14 is due to the aggregate $[(Bu_4N)_4Cu_2(Mo_6O_{20}C_7H_4N)_4]^{4-}$ consisting of $[Bu_4N]^+$, Cu^{2+}, and $[Mo_6O_{20}C_7H_4N]^{3-}$. Similarly, the signal at m/z 767.65 is assigned to the aggregate $[(Bu_4N)_2Cu_2(Mo_6O_{20}C_7H_4N)_4]^{6-}$ (Table 1). The existence of the fragment of **2** shows that the

Table 1. ESI results of Compound 2

m/z	aggregate	calcd m/z	rel. intens. (%)
1272.14	$[(Bu_4N)_4Cu_2(Mo_6O_{20}C_7H_4N)_4]^{4-}$	1271.97	12
767.65	$[(Bu_4N)_2Cu_2(Mo_6O_{20}C_7H_4N)_4]^{6-}$	767.16	10
1360.83	$[(Bu_4N)_3H(Mo_6O_{20}C_7H_4N)_2]^{2-}$	1361.94	5
998.40	$[H_2(Mo_6O_{20}C_7H_4N)]^-$	999.76	5
1240.66	$[(Bu_4N)H(Mo_6O_{20}C_7H_4N)]^-$	1241.21	100

formation and disassembly process are in dynamic equilibrium in the solution. Then through changing the environment of the solution, such as the pH value and temperature, we can control the formation and disassembly process. The research is currently under study in our laboratory.

Furthermore, compound **2** can further self-assemble into vesicular-like supramolecular aggregates at nanoscale in polar solvents. Contrarily, the solution behavior of **1** is completely different, which stays as discrete ions in polar solvents. Static and dynamic laser light-scattering (SLS and DLS) techniques were used to characterize the aggregates formed in toluene/acetone solutions (toluene vol%: 1/8) of compound **2**. The scattered intensity from compound **2** solution keeps increasing for the next 27 days before reaching equilibrium, suggesting a slow and continuous association process. A typical CONTIN analysis[27] from the DLS study shows that large aggregates have an average hydrodynamic radius (R_h) of 116 ± 6 nm with a narrow size distribution, and this value does not change obviously within 40 days (Figure 4). The SLS measurement indicates that the aggregates have an average radius of gyration (R_g) of 123 ± 6 nm. The ratio of R_h/R_g is ~1, suggesting that the aggregates have a vesicular-like structure.[7] The hollow spherical structures were further confirmed by TEM results

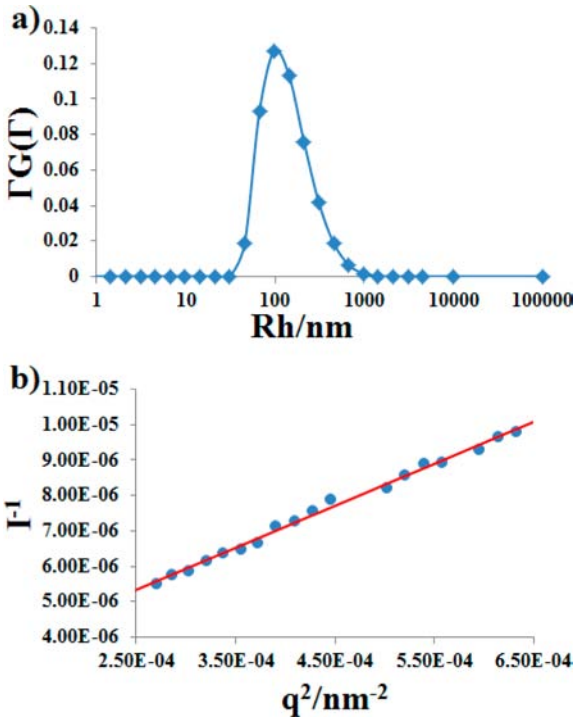

Figure 4. Light-scattering results of the solution of **2**. The concentration of the solution is 0.5 mg/mL in the mixture of toluene and acetone (toluene vol% = 1/8). (a) CONTIN analysis on the DLS study of the solution of **2**; (b) SLS study of the same solution in (a).

(Figures 5a and b). An X-ray energy dispersive spectrum (EDS) was collected from the aggregates on the copper grid, and the

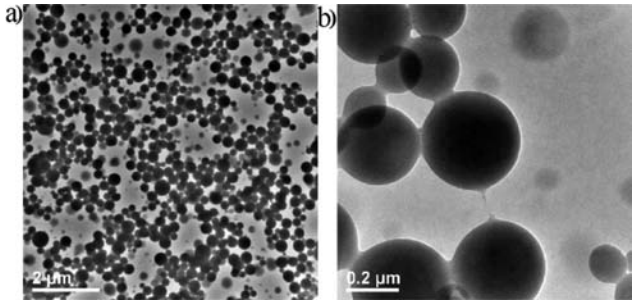

Figure 5. (a) TEM images of the uniform aggregates of **2**. (b) Zoomed-in images of (a). The spherical structures can be clearly observed even when they are highly overlapped, which confirms the hollow properties of the features.

peak appearing at 17.4 KeV indicates the existence of molybdenum. The zeta-potential result is −36.6 mV, suggesting that the aggregates are negatively charged. The hollow spherical structure, together with the slow, continuous assembly and the time-independent assembly sizes, are characteristic features for the self-assembly of various macro-ions into vesicle-like, single-layered, blackberry-type structures in polar solvents,[7] as shown schematically in Figure 6.

The aggregate size increases with decreasing solvent polarity, i.e., with more toluene content. When the content of toluene is >33% in the solvent, no large aggregates can be observed. This is likely because the countercations are closely associated with the macroclusters to make them almost uncharged in a less polar environment, and therefore the macroclusters are not

dx.doi.org/10.1021/ja408228b | J. Am. Chem. Soc. 2013, 135, 17155−17160

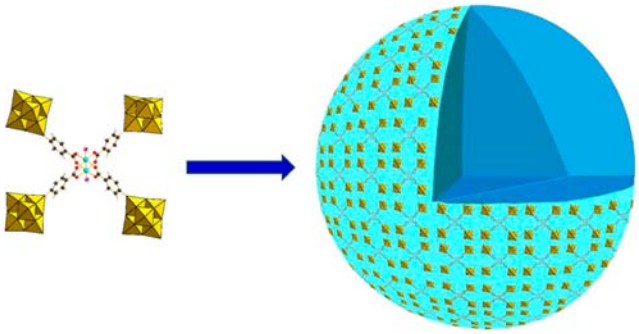

Figure 6. The blackberry model of **2**. The yellow polyhedron represents hexamolybdate anion. Atom coding: copper (cyanine), oxygen (red), carbon (black), hydrogen (gray), solvent molecule (purple). The single layer hollow spherical structure represents the blackberry structure formed by **2**.

macro-ions anymore. On the other hand, no self-assembly occurs in acetonitrile (very high polarity) due to the strong electrostatic repulsions among the highly charged macro-ions (Figure 7). This observation can rule out the possibility that the

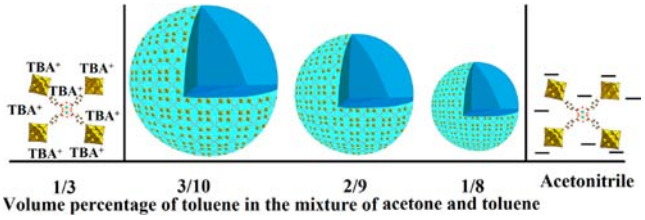

Figure 7. Complete transition of single macro-anions—blackberry structures—macroanions is achieved by simply adjusting the solvent quality of the compound **2** solution.

aggregates are bilayer regular vesicles formed via hydrophobic interactions. In such a case the vesicle formation should be promoted in a more polar solvent. The fact that the aggregates are obviously charged also excludes the possibility that the aggregates are reverse vesicles. Therefore, it is safe to conclude that compound **2** forms blackberry-type structures. The current observations indicate the surface charge plays a critical role in the blackberry formation process. Overall, the self-assembly cannot occur when the clusters carry too high or too low charge.[28] Moreover, within the solvent polarity range that allows the blackberry formation, the assembly size displays a linear relationship with $1/\varepsilon$ (ε being the dielectric constant of solvent) (Figure S5), which is a quite important character for charge-regulated self-assembly processes.[29]

4. CONCLUSION

In summary, a novel hexamolybdate-based paddle-wheel macrocluster has been successfully synthesized by the use of organoimido derivatives of hexamolybdate as building blocks and copper ions as linkers. Such macroclusters can further self-assemble into vesicular-like supramolecular aggregates at nanoscale, while the subunits cannot. The results demonstrate this strategy is a feasible and effective approach with more controllability and designability to fabricate such POM-macrostructures with interesting properties. This way can be extended via choosing various transition metals and functional ligands within POM-organic derivatives. It is believed that this work will be of significance in exploiting the POM-based macrostructures.

■ ASSOCIATED CONTENT

Supporting Information

IR spectra, distribution of the size of the vesicles, structural figure with probability ellipsoids, scattering intensity monitoring results, light-scattering results, EDS results and the linear relationship between R_h and $1/\varepsilon$. Crystallographic data. This material is available free of charge via the Internet at http://pubs.acs.org.

■ AUTHOR INFORMATION

Corresponding Authors

tliu@uakron.edu
yonggewei@tsinghua.edu.cn
wangy@pku.edu.cn

Author Contributions

⊥Y.Z. and P.Y. contributed equally to this work.

Notes

The authors declare no competing financial interest.

■ ACKNOWLEDGMENTS

T.L. acknowledges support from NSF CHM1305756. Y. Wei acknowledges support from NSFC (Nos. 21225103 and 21221062), THSJZ, Tsinghua University Initiative Foundation Research Program No. 20101081771, and the open project of the Key Laboratory of Polyoxometalate Science of the Ministry of Education of China. Y. Wang acknowledges support from MOST No. 2011CB808702.

■ REFERENCES

(1) (a) *Structure and Bonding: Molecular Machines and Motors*; Sauvage, J.-P., Ed.; Springer-Verlag: Heidelberg, 2001, p 99 and references therein. (b) *Structure and Bonding: Molecular Self-Assembly: Organic Versus Inorganic Approaches*; Fujita, M., Ed.; Springer-Verlag: Heidelberg, 2000, p 96 and references therein. (c) *Supramolecular Chemistry: Concept and Perspectives*; Lehn, J. M.; VCH: New York, 1995. (d) Whitesides, G. M.; Grzybowski, B. *Science* **2002**, *295*, 2418. (e) Matthew, C. T.; Stoddart, J. F. *Acc. Chem. Res.* **1997**, *30*, 393. (f) Lindsey, J. S. *New. J. Chem.* **1991**, *15*, 153. (g) Reinhoudt, D. N.; Crego-Calama, M. *Science* **2002**, *295*, 2403.

(2) (a) Stang, P. J.; Olenyuk, B. *Acc. Chem. Res.* **1997**, *30*, 502. (b) Leininger, S.; Olenyuk, B.; Stang, P. J. *Chem. Rev.* **2000**, *100*, 853. (c) Seidel, S. R.; Stang, P. J. *Acc. Chem. Res.* **2002**, *35*, 972. (d) Northrop, B. H.; Yang, H.-B.; Stang, P. J. *Chem. Commun.* **2008**, 5896.

(3) (a) Caulder, D. L.; Raymond, K. N. *Acc. Chem. Res.* **1999**, *32*, 975. (b) Holliday, B. J.; Mirkin, C. A. *Angew. Chem., Int. Ed.* **2001**, *40*, 2022. (c) Fujita, M.; Tominaga, M.; Hori, A.; Therrien, B. *Acc. Chem. Res.* **2005**, *38*, 369. (d) Lee, S. J.; Hupp, J. T. *Coord. Chem. Rev.* **2006**, *250*, 1710. (e) Tranchemontagne, D. J.; Ni, Z.; O'Keeffe, M.; Yaghi, O. M. *Angew. Chem., Int. Ed.* **2008**, *47*, 5136.

(4) Selected recent examples of coordination-driven self-assembly: (a) Zhang, Z. M.; Yao, S.; Li, Y. G.; Clérac, R.; Lu, Y.; Su, Z. M.; Wang, E. B. *J. Am. Chem. Soc.* **2009**, *131*, 14600. (b) Sigmon, G. E.; Ling, J.; Unruh, D. K.; Moore-Shay, L.; Ward, M.; Weaver, B.; Burns, P. C. *J. Am. Chem. Soc.* **2009**, *131*, 16648. (c) Li, J. R.; Zhou, H. C. *Angew. Chem., Int. Ed.* **2009**, *48*, 8465. (d) Li, J. R.; Timmons, D. J.; Zhou, H. C. *J. Am. Chem. Soc.* **2009**, *131*, 6368. (e) Kong, X. J.; Wu, Y. L.; Long, L. S.; Zheng, L. S.; Zheng, Z. P. *J. Am. Chem. Soc.* **2009**, *131*, 6918. (f) Lu, Z.; Knobler, C. B.; Furukawa, H.; Wang, B.; Liu, G. N.; Yaghi, O. M. *J. Am. Chem. Soc.* **2009**, *131*, 12532. (g) Lee, J.; Ghosh, K.; Stang, P. J. *J. Am. Chem. Soc.* **2009**, *131*, 12028. (h) Ghosh, K.; Hu, J. M.; White, H. S.; Stang, P. J. *J. Am. Chem. Soc.* **2009**, *131*, 6695.

(5) (a) Müller, A.; Shah, S. Q. N.; Bögge, H.; Schmidtmann, M. *Nature* **1999**, *397*, 48. (b) Müller, A.; Das, S. K.; Kögerler, P.; Bögge, H.; Schmidtmann, M.; Trautwein, A. X.; Schunemann, V.; Krickemeyer, E.; Preetz, W. *Angew. Chem., Int. Ed.* **2000**, *39*, 3414. (c) Zhang, S.-W.; Wei, Y.-G.; Yu, Q.; Shao, M.-C.; Tang, Y.-Q. *J. Am. Chem. Soc.* **1997**, *119*, 6440.

(6) (a) Sadakane, M.; Dickman, M. H.; Pope, M. T. *Angew. Chem., Int. Ed.* **2000**, *39*, 2914. (b) Kortz, U.; Savelieff, M. G.; Bassil, B. S.; Dickman, M. H. *Angew. Chem., Int. Ed.* **2001**, *40*, 3384. (c) Kortz, U.; Hussain, F.; Reicke, M. *Angew. Chem., Int. Ed.* **2005**, *44*, 3773.

(7) (a) Liu, T.; Diemann, E.; Li, H.; Dress, A. W. M.; Müller, A. *Nature* **2003**, *426*, 59. (b) Liu, G.; Liu, T. J. *Am. Chem. Soc.* **2005**, *127*, 6942. (c) Liu, T.; Imber, B.; Diemann, E.; Liu, G.; Cokleski, K..; Li, H..; Chen, Z.; Müller, A. *J. Am. Chem. Soc.* **2006**, *128*, 15914. (d) Zhang, J.; Li, D.; Liu, G.; Glover, K. J.; Liu, T. *J. Am. Chem. Soc.* **2009**, *131*, 15152. (e) Liu, T.; Langston, M. L. K.; Li, D.; Pigga, J. M.; Pichon, C.; Todea, A. M.; Müller, A. *Science* **2011**, *331*, 1590.

(8) (a) Song, Y.-F.; Long, D.-L.; Cronin, L. *Angew. Chem., Int. Ed.* **2007**, *46*, 3900. (b) Pradeep, C. P.; Long, D. L.; Newton, G. N.; Song, Y. F.; Cronin, L. *Angew. Chem., Int. Ed.* **2008**, *47*, 4388. (c) Wang, L.; Zhu, L.; Yin, P.; Fu, W.; Chen, J.; Hao, J.; Xiao, F.; Lv, C.; Zhang, J.; Shi, L.; Wei, Y. *Inorg. Chem.* **2009**, *48*, 9222. (d) Johnson, B. J. S.; Schroden, R. C.; Zhu, C. C.; Stein, A. *Inorg. Chem.* **2001**, *40*, 5972.

(9) (a) Mialane, P.; Dolbecq, A.; Sécheresse, F. *Chem. Commun.* **2006**, 3477. (b) Dolbecq, A.; Mialane, P.; Lisnard, L.; Marrot, J.; Sécheresse, F. *Chem.—Eur. J.* **2003**, *9*, 2914. (c) Mialane, P.; Dolbecq, A.; Rivière, E.; Marrot, J.; Sécheresse, F. *Eur. J. Inorg. Chem.* **2004**, 33. (d) Dolbecq, A.; Draznieks, C. M.; Mialane, P.; Marrot, J.; Férey, G.; Sécheresse, F. *Eur. J. Inorg. Chem.* **2005**, 3009. (e) Zheng, S. T.; Zhang, J.; Yang, G. Y. *Angew. Chem., Int. Ed.* **2008**, *47*, 3909.

(10) (a) Bar-Nahum, I.; Cohen, H.; Neumann, R. *Inorg. Chem.* **2003**, *42*, 3677. (b) Johnson, B. J. S.; Schroden, R. C.; Zhu, C. C.; Young, V. G., Jr.; Stein, A. *Inorg. Chem.* **2002**, *41*, 2213.

(11) (a) Han, J. W.; Hardcastle, K. I.; Hill, C. L. *Eur. J. Inorg. Chem.* **2006**, 2598. (b) Han, J. W.; Hill, C. L. *J. Am. Chem. Soc.* **2007**, *129*, 15094.

(12) (a) Song, Y.-F.; McMillan, N.; Long, D.-L.; Kane, S.; Malm, J.; Riehle, M. O.; Pradeep, C. P.; Gadegaard, N.; Cronin, L. *J. Am. Chem. Soc.* **2009**, *131*, 1340. (b) Song, Y.-F.; Abbas, H.; Ritchie, C.; McMillian, N.; Long, D.-L.; Gadegaard, N.; Cronin, L. *J. Mater. Chem.* **2007**, *17*, 1903.

(13) Favette, S.; Hasenknopf, B.; Vaissermann, J.; Gouzerh, P.; Roux, C. *Chem. Commun.* **2003**, 2664.

(14) Kang, J.; Xu, B. B.; Peng, Z. H.; Zhu, X. D; Wei, Y. G.; Powell, D. R. *Angew. Chem., Int. Ed.* **2005**, *44*, 6902.

(15) (a) Hill, C. L. Ed. *Chem. Rev.* **1998**, *98*, 1. (b) Pope, M. T. In *Comprehensive Coordination Chemistry II*; McCleverty, J. A., Meyer, T. J., Eds.; Elsevier: Oxford, 2004; Vol. 4, p 635. (c) Hill, C. L. In *Comprehensive Coordination Chemistry II*; McCleverty, J. A., Meyer, T. J., Eds.; Elsevier: Oxford, 2004; Vol. 4, p 679. (d) Moffat, J. B. *Metal-Oxygen Clusters: The Surface and Catalytic Properties of Heteropoly Oxometalates*; Kluwer Academic/Plenum Publishers: New York, 2001.

(16) (a) Pope, M. T.; Müller, A. *Polyoxometalates Chemistry From Topology via Self-Assembly to Application*; Kluwer Academic Publishers: Dordrecht, 2001. (b) Yamase, T.; Pope, M. T. *Polyoxometalate Chemistry for Nano-Composite Design*; Kluwer Academic/Plenum Publishers: New York, 2002. (c) Müller, A.; Roy, S. *The Chemistry of Nanomaterials: Synthesis, Properties and Applications*; Wiley-VCH: Weinheim, Germany, 2004. (d) Long, D.-L.; Burkholder, E.; Cronin, L. *Chem. Soc. Rev.* **2007**, *36*, 105.

(17) (a) González-Rodríguez, D.; van Dongen, J. L. J.; Lutz, M.; Spek, A. L.; Schenning, A. P. H. J.; Meijer, E. W. *Nat. Chem.* **2009**, *1*, 151. (b) Stevens, M. J. *Phys. Rev. Lett.* **1999**, *82*, 101. (c) Yan, Y.; Chan-Park, M. B.; Zhang, Q. *Small* **2007**, *3*, 24. (d) Liu, T. *Langmuir* **2009**, *26*, 9202. (e) Yan, H.; Park, S. H.; Finkelstein, G.; Reif, J. H.; LaBean, T. H. *Science* **2003**, *301*, 1882.

(18) This compound was initially synthesized by E. A. Maatta et al. See: Moore, A. R. Ph.D. Dissertation, Kansas State University, Mahattan, KS, 1998.

(19) There were 672 structures, including binuclear copper paddle-wheel fragment, obtained from CCDC (Cambridge Crystallographic Data Centre).

(20) (a) Wu, P.; Li, Q.; Ge, N.; Wei, Y.; Wang, Y.; Wang, P.; Guo, H. *Eur. J. Inorg. Chem.* **2004**, 2819. (b) Wei, Y.; Xu, B.; Barnes, C. L.; Peng, Z. *J. Am. Chem. Soc.* **2001**, *123*, 4083.

(21) Brese, N. E.; O'Keeffe, M. *Acta Crystallogr.* **1991**, *B47*, 192.

(22) Doyle, A.; Felcman, J.; Gambardella, M.; Verani, C. N.; Tristão, M. *Polyhedron* **2000**, *19*, 2621.

(23) (a) Du, Y.; Rheingold, A. L.; Maatta, E. A. *J. Am. Chem. Soc.* **1992**, *114*, 345. (b) Strong, J. B.; Yap, G . P. A.; Ostrander, R.; Liable-Sands, L. M.; Rheingold, A. L.; Thouvenot, R.; Gouzerh, P.; Maatta, E. A. *J. Am. Chem. Soc.* **2000**, *122*, 639.

(24) (a) Errington, R. In *Polyoxometalates Chemistry: From Topology Via Self-Assembly to Applications*; Pope, M. T., Müller, A., Eds.; Kluwer Academic Publisher: Dordrecht: Boston, 2002; pp 7−22. (b) Proust, A.; Thouvenot, R.; Chaussade, M.; Robert, F.; Gouzerh, P. *Inorg. Chim. Acta* **1994**, *224*, 81.

(25) (a) Mülliken, R. S. *J. Am. Chem. Soc.* **1952**, *74*, 811. (b) Mülliken, R. S.; Person, W. B. *Molecular Complexes:, A Lecture and Reprint*; Wiley: New York, 1969. (c) Foster, R. *Organic Charge-Transfer Complexes*; Academic Press: New York, 1969.

(26) Grodzicki, A.; Sztyk, E.; Wojtczak, A.; Wrzeszcz, G.; Pazderski, L.; Muziot, T. *Polyhedron* **1999**, *18*, 519.

(27) Provencher, S. W. *Comput. Phys. Commun.* **1982**, *27*, 229.

(28) Kistler, M. L.; Bhatt, A.; Liu, G.; Casa, D.; Liu, T. *J. Am. Chem. Soc.* **2007**, *129*, 6453.

(29) Verhoeff, A. A.; Kistler, M. L.; Bhatt, A.; Pigga, J.; Groenewold, J.; Klokkenburg, M.; Veen, S.; Roy, S.; Liu, T.; Kegel, W. K. *Phys. Rev. Lett.* **2007**, *99*, 066104.